Nuclear Instruments and Methods in Physics Research A 361 (1995) 306–316

NUCLEAR INSTRUMENTS & METHODS IN PHYSICS RESEARCH Section A

ELSEVIER

Background subtraction from in-beam HPGe coincidence data sets

D.C. Radford

AECL Research, Chalk River Laboratories, Chalk River, Ontario, Canada K0J 1J0

Received 29 November 1994

Abstract

Algorithms for the subtraction of backgrounds from γ–γ matrices and higher-fold data sets, obtained from in-beam HPGe coincidence experiments with heavy-ion-induced nuclear reactions, are described. The backgrounds are parameterized as the cross-products of lower-dimensional projections of the data and a one-dimensional background spectrum. A novel method of correcting for a mixture of different reaction channels in the complete data set, by making use of one or more gates on background channels in the energy region of the "E2 bump", is presented. In many cases, this new method provides a significantly better description of the background.

1. Introduction

Modern HPGe detector arrays have revolutionized in-beam γ-ray studies, especially for high-spin nuclear structure physics with heavy-ion fusion-evaporation reactions. In the analysis of data from such arrays, one often creates two-dimensional histograms from double-coincidence data, or three-dimensional histograms from triple-coincidence data, and then proceeds to set "gates", i.e. specify energies for all but one of the axes and inspect the projection onto the remaining axis. More sophisticated procedures (e.g. Refs. [1,2]) may attempt to perform least-squares fits directly to the multi-fold data to extract coincident peak areas and energies. In either case, it is usually necessary to correct the data for background counts underlying the peaks in the gate spectrum or fitted region, arising from both Compton-scattered γ-rays and quasicontinuum transitions.

One common method for correcting for the background underlying a gate on a peak is to set additional gates on background regions near the peak, and subtract a normalized fraction of the resulting projection from that obtained with the primary gate. (In three- and higher-fold data, combinations of peak and background gates are used.) In practise, however, it is often not possible to find a background region free from weak contaminant peaks. This procedure also introduces more statistical uncertainty into the results than is strictly necessary, since the background spectrum has a similar number of counts to the primary (peak) spectrum. In addition, this method does not remove all of the background counts from the resulting spectrum; i.e. the result still contains counts from Compton-scattered γ-rays and quasicontinuum transitions in true coincidence with the peak. Therefore, when a direct least-squares analysis of the peaks in a multi-fold data set is desired, this procedure cannot be used, and some other method of determining the background must be found.

A second method that is commonly used for two-dimensional data is to subtract a fraction of the total one-dimensional projection from the gated spectrum, normalized so that the total counts subtracted corresponds to an estimate of the background counts in the gate. This procedure does not have the problem of introducing additional statistical uncertainty, but still does not remove coincident background counts from the spectrum. Generalisations of this method to higher folds have also been made (e.g. Ref. [3]).

Palameta and Waddington [4] have reported a method of subtracting the background directly from two-dimensional γ–γ histograms ("matrices"). The present paper reports a prescription similar to that of Ref. [4] but somewhat simpler. The limitations of this and other prescriptions are discussed. In particular, for nuclei populated in heavy-ion fusion-evaporation reactions, correlations of the background with the reaction channel (i.e. different residual nuclei) can pose a significant problem. We therefore present an extension to the basic method which allows a correction for the different reaction channels typically present in a data set. Extensions to three- and higher-dimensional data sets are also given.

2. Principles of the method

In order to give a simple description of the method, we will begin by discussing two-dimensional (2D) γ–γ data sets. Extensions to higher folds will be presented later.

Analysis of a γ–γ data set will typically begin with generating a "matrix", or 2D histogram of counts vs.

Elsevier Science B.V.
SSDI 0168-9002(95)00184-0

energy vs. energy. This matrix is then usually symmetrised, so that the two energy axes are equivalent.

Let the counts in such a data set be represented by M_{ij}, where i and j indices are the channels corresponding to the γ-ray energies. The one-dimensional (1D) projection of the matrix is then

$$P_i = \sum_j M_{ij}.$$

Let us divide the counts in this projection into a "background" spectrum b_i and a "peak" spectrum p_i, such that

$$P_i = b_i + p_i.$$

The details of how this is done need not greatly concern us here; the sensitivity of the resulting 2D background to this partition is addressed below. For now, it will be sufficient to imagine that an experimenter "draws" the 1D background b_i below the peaks in the projection in order to define the two spectra.

The second procedure mentioned above in the introduction (subtracting part of the 1D projection) would then correspond to subtracting the 2D background

$$B_{ij} = \frac{1}{T} b_i P_j$$

$$= \frac{1}{T}\left(b_i b_j + b_i p_j\right), \tag{1}$$

where

$$T = \sum_{ij} M_{ij} = \sum_i P_i \tag{2}$$

is the total number of counts in the matrix. This 2D background is not symmetric, and would be used for gates set on the i-axis and projected onto the j-axis.

As mentioned above, this does not remove the background counts in coincidence with the peak of the gate. In

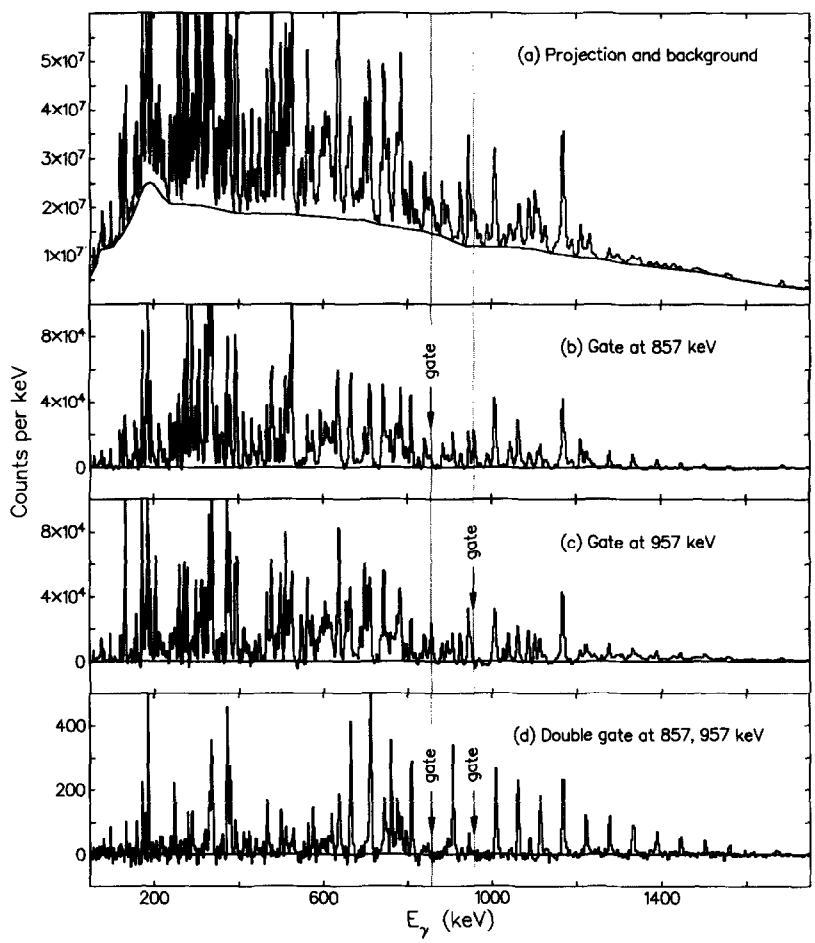

Fig. 1. Spectra from the reaction ^{124}Sn + ^{30}Si at 158 MeV, studied with the EUROGAM 1 spectrometer [5]. Shown are: (a) the total 1D projection and background spectra; (b), (c) two background-subtracted gated spectra from a 2D matrix; and (d) background-subtracted double-gated spectrum generated by setting the two gates together on a 3D cube and projecting the result onto the third dimension.

order to do this, and to maintain symmetry, we extend the procedure and use the following 2D background:

$$B_{ij} = \frac{1}{T}\left(b_i b_j + b_i p_j + p_i b_j\right) = \frac{1}{T}\left(P_i P_j - p_i p_j\right). \quad (3)$$

Fig. 1 illustrates the use of this background for data from the reaction ^{124}Sn + ^{30}Si at 158 MeV, studied with the EUROGAM 1 spectrometer [5]. Shown are the total 1D projection and "drawn" background spectra, together with two background-subtracted gates on a 2D matrix. It is remarkable how well such a simple background is able to represent the true observed background. Also shown is a background-subtracted spectrum generated by setting both of the two gates together on a 3D cube and projecting the result onto the third dimension; this is discussed in Section 5, where the extension of Eq. (3) to three-and higher-folds is presented.

For the study of E_γ–E_γ correlations in γ–γ coincidences, the COR [6] method can be used to generate a background with the same total number of counts (T) as the matrix; it corresponds to the simple 2D background

$$B_{ij}^{\mathrm{COR}} = \frac{1}{T} P_i P_j.$$

No net counts remain in the matrix after this subtraction. The technique presented here removes from such a 2D background the peak–peak part of the projection cross-product, and can in that sense be considered a refinement of the COR treatment.

Our method is also related to that of Palameta and Waddington [4]. In our nomenclature, their 2D background can be rewritten as:

$$B_{ij}^{\mathrm{PW}} = \frac{1}{S}\left(b_i P'_j + P'_i b_j - A b_i b_j\right).$$

Here the 1D spectrum P'_i is the projection of the matrix

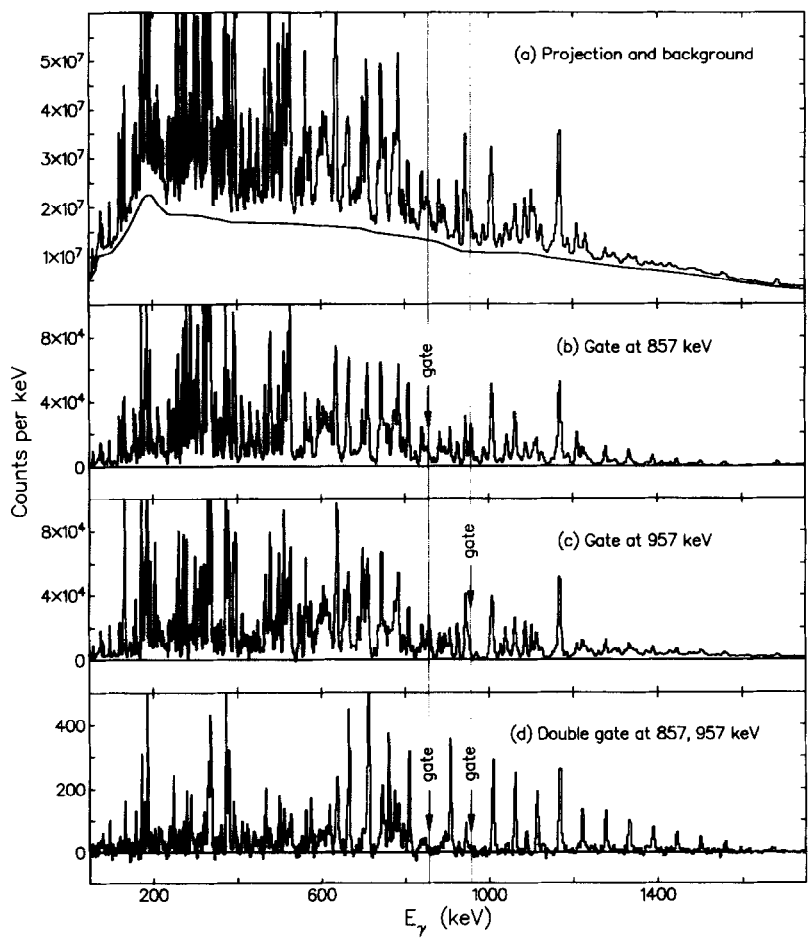

Fig. 2. Spectra from the same data set and identical gates as for Fig. 1, but using a 1D background spectrum which has been renormalized by a factor of 0.9. Shown are: (a) the total 1D projection and renormalized background spectra; (b), (c) background-subtracted gated spectra from a 2D matrix; and (d) background-subtracted double-gated spectrum.

for the set K of all channels for which $P_j - b_j$ is zero within statistical errors (i.e. all channels containing no significant peaks),

$$P'_i = \sum_{j \in K} M_{ij},$$

and the constants S and A are defined as

$$S = \sum_i P'_i,$$

$$A = \sum_{i \in K} P'_i / S.$$

If we expand the set K to include *all* channels of the j-axis, then we get

$P'_i = P_i$,

$S = T$,

$A = 1$,

and the background of Palameta and Waddington reduces to that of Eq. (3).

3. Sensitivity of the method to the background spectrum

The use of Eq. (3) requires the definition of the background spectrum b_i. One can define this spectrum simply by drawing a piecewise-linear curve below the visible peaks in the total projection. Since this is clearly a subjective procedure, it is important to examine the sensitivity of the final result to this 1D background spectrum.

A simple way of doing this is to define an alternative background spectrum, b'_i, for example by multiplying b_i by a factor 0.9. Thus we obtain

$$b'_i = 0.9 b_i,$$

$$p'_i = P_i - b'_i$$

$$= p_i + 0.1 b_i,$$

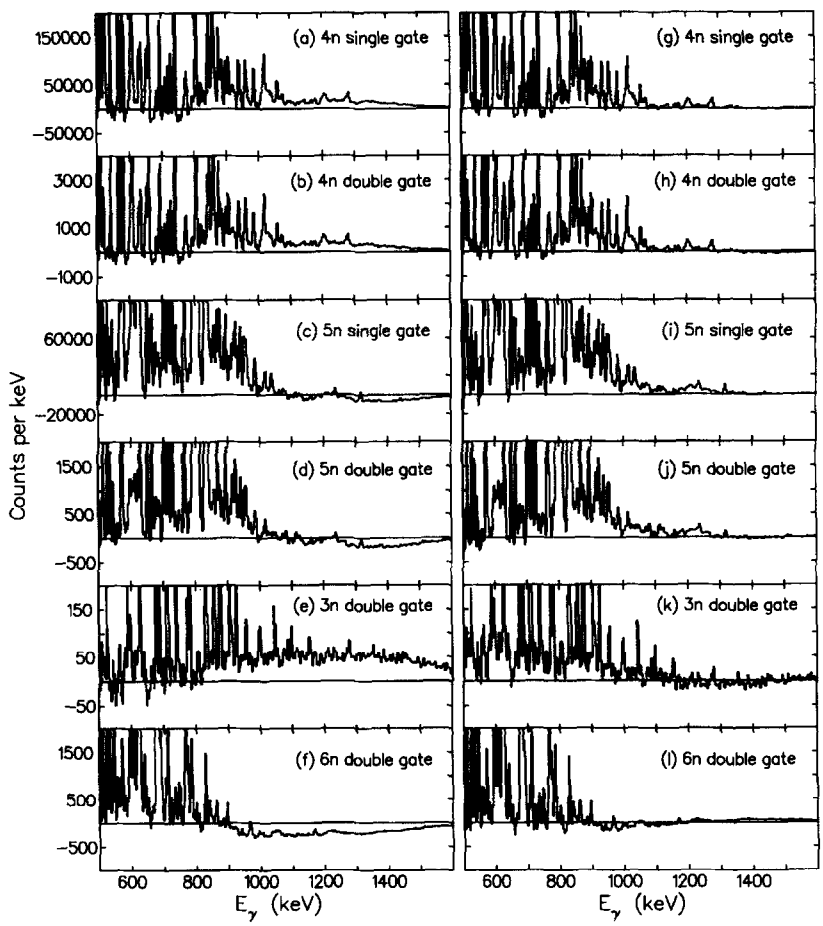

Fig. 3. Gated spectra from the reaction of ^{114}Cd with 210 MeV ^{48}Ca, taken with the EUROGAM 1 spectrometer. The background has been subtracted using the standard procedure of Eq. (3) (left-hand side, (a)–(f)), or using the improved procedure of Eq. (11) (right-hand side, (g)–(l)). (a), (g): Gate on the 443 keV transition in ^{158}Er. (b), (h): Double gate on the 443 and 522 keV transitions in ^{158}Er. (c), (i): Gate on the 527 keV transition in ^{157}Er. (d), (j): Double gate on the 527 and 622 keV transitions in ^{157}Er. (e), (k): Double gate on the 464 and 556 keV transitions in ^{159}Er. (f), (l): Double gate on the 452 and 543 keV transitions in ^{156}Er.

$$B'_{ij} = \frac{1}{T}\left(P_iP_j - p'_ip'_j\right)$$

$$= \frac{1}{T}\left(P_iP_j - p_ip_j - 0.1p_ib_j - 0.1b_ip_j + 0.01b_ib_j\right)$$

$$= B_{ij} - \frac{0.1}{T}\left(p_ib_j + b_ip_j - 0.1b_ib_j\right). \quad (4)$$

Since the bulk of the counts are in the P_iP_j term, rather than the p_ip_j term, this renormalization of b_i has only a relatively minor effect on the resulting 2D background. This can be illustrated by taking the same gates as in Fig. 1, but now using this renormalized background; these spectra are shown in Fig. 2. It can be seen that even a relatively large change in b_i has quite a small effect, especially for the triples spectrum.

As can be seen from Eq. (4), a change in b_i has a very small effect on the b_ib_j term of B_{ij}. However, the terms in p_ib_j and b_ip_j are more sensitive. Thus, for gates with very small peak-to-background ratios, a poorly-defined 1D background will result in strong peaks of the total projection being oversubtracted or undersubtracted.

Attempts have been made to develop techniques to automatically generate b_i from P_i. These have not been very successful, in that the subjective technique of removing the peaks by hand generally gives results at least as reliable as the automatic methods.

Experience has shown that including in b_i the shoulders and/or peaks arising from (n, n'γ) events in the HPGe detector or surrounding material will generally result in an improved background subtraction. Similarly, some experiments produce X-rays in strong coincidence with virtually all peaks of the spectrum, due to internal conversion of γ-rays. In such cases, leaving the X-ray peaks in the b_i spectrum will remove an average X-ray coincident intensity from the gated spectra.

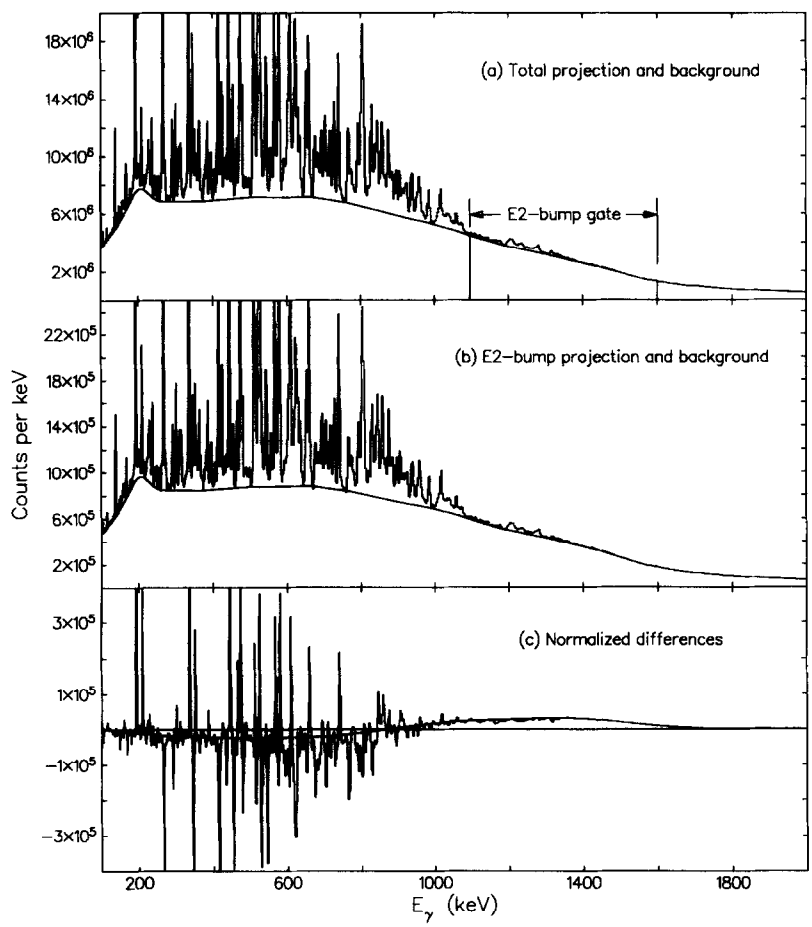

Fig. 4. Illustration of the E2-bump correction for improved background subtraction. The spectra are from the reaction of ^{114}Cd with 210 MeV ^{48}Ca, taken with the EUROGAM 1 spectrometer. Shown are: (a): Total 1D projection and background. Also shown are the limits of the gate set on the E2-bump region, used to produce the spectrum in (b). (b): Gated E2-bump 1D projection and background. (c): Normalized differences of the projections and backgrounds of parts (b) and (a). The normalization factor was chosen to be the ratio of the total counts in the projections, i.e. to give zero net counts in the projection difference.

4. Correction for multiple reaction channels

When nuclei are produced at high spin with heavy-ion fusion-evaporation reactions, there are usually at least two or three strongly populated residues. For example, in the bombardment of ^{114}Cd with 210 MeV ^{48}Ca, the dominant reaction channels are ^{114}Cd(^{48}Ca, 4n)^{158}Er and ^{114}Cd(^{48}Ca, 5n)^{157}Er, while weaker reaction channels include 3n and 6n evaporation, and pxn evaporation.

If a residue is produced at higher spin, then more of the total energy is carried as rotational energy, so that less of the energy brought in by the reaction was available for the evaporation of particles. Thus, in the above example, ^{158}Er is generally produced with more angular momentum than ^{157}Er. This extra angular momentum must then be removed by γ-ray emission subsequent to the neutron evaporation, resulting in a higher average γ-ray multiplicity. For collectively-rotating nuclei, most of the extra γ-rays contribute to a quasicontinuum "E2 bump" in the energy region between 1 and 1.5 MeV. Consequently, the shape of this quasicontinuum γ-ray spectrum also differs between reaction channels. In the type of background subtraction described here, the quasicontinuum is considered to be part of the "background" we are subtracting, and this will give rise to reaction-channel-dependent effects.

This can be seen in Fig. 3, where spectra from gates on strong $^{156-159}$Er γ-ray transitions are shown. The spectra on the left have been background-subtracted with the procedure of Eq. (3). In the region between about 1000 and 1500 keV there are serious problems with the background; the 3n- and 4n-evaporation spectra are undersubtracted, while the 5n and 6n are oversubtracted. Since we are subtracting an average background, the reaction-channel dependence of the E2-bump strength is a serious problem.

The effect that gives rise to this problem, however, also points the way to a solution. It is evident that setting a gate on background channels in the region of the E2-bump will effectively distinguish the reaction channel of strong peaks in the spectrum. It should then be possible to use this information to add a correction term to the background subtraction.

This is illustrated in Fig. 4. The top panel shows the total 1D projection and background from the data set of Fig. 3. Also shown is a wide gate on the E2-bump region of the spectrum, from 1100 to 1600 keV, chosen to avoid strong peaks. When this gate is applied to the 2D data, the projection spectrum shown in the middle panel results. A 1D background can be drawn for this E2-bump-gated spectrum in the same way as for the total projection. In the bottom panel, the E2-bump projection has had a fraction of the total projection subtracted, with a normalization factor chosen to give a net counts of zero in the difference spectrum. The difference in the background spectra, with the same normalization coefficient, is also shown. The positive (negative) peaks in the difference spectrum correspond to transitions from the 3n and 4n (5n and 6n) evaporation residues. It is also evident that the E2-bump is more intense in the E2-bump-gated projection than in the total projection.

Let E be the set of channels included in the E2-bump gate(s), so that the E2-bump projection spectrum is

$$S_i = \sum_{j\in E} M_{ij},$$

with a total counts of

$$C = \sum_i S_i = \sum_{i\in E} P_i.$$

Let us divide the counts in the E2-bump projection into background and peaks,

$$S_i = s_i + t_i,$$

and define the difference spectra of Fig. 4c as

$$D_i = S_i - \frac{C}{T}P_i,$$

$$e_i = t_i - \frac{C}{T}b_i,$$

$$d_i = D_i - e_i$$

$$= s_i - \frac{C}{T}p_i.$$

In order to simplify the discussion which follows, we consider an experiment where the two primary reactions are (HI, xn) and (HI, $(x+1)$n). Let the 2D data, total projection and background be:

$$M_{ij} = M^{\mathrm{a}}_{ij} + M^{\mathrm{b}}_{ij},$$

$$P_i = P^{\mathrm{a}}_i + P^{\mathrm{b}}_i,$$

$$b_i = b^{\mathrm{a}}_i + b^{\mathrm{b}}_i,$$

where the superscripts a and b represent spectra that would be obtained from pure (HI, xn) and (HI, (x + 1)n) data sets, respectively. We define

$$T^n = \sum_i P^n_i,$$

$$S^n_i = \sum_{j\in E} M^n_{ij},$$

$$C^n = \sum_i S^n_i,$$

where n = a, b. We also obtain

$$T = T^{\mathrm{a}} + T^{\mathrm{b}},$$

$$S_i = S^{\mathrm{a}}_i + S^{\mathrm{b}}_i,$$

etc.

If the E2-bump gate on each of the individual reaction channels is well-reproduced by the background, then the

spectra S_i^n can be well represented by a fraction of the total projections P_i^n,

$$S_i^n = \frac{C^n}{T^n} P_i^n.$$

We therefore obtain

$$\begin{aligned} D_i &= S_i - \frac{C}{T} P_i \\ &= S_i^a + S_i^b - \frac{C}{T}\left(P_i^a + P_i^b\right) \\ &= \frac{C^a}{T^a} P_i^a + \frac{C^b}{T^b} P_i^b - \frac{C^a + C^b}{T^a + T^b}\left(P_i^a + P_i^b\right) \\ &= \frac{C^a T^b - C^b T^a}{T T^a T^b}\left(T^b P_i^a - T^a P_i^b\right) \quad (5) \\ &= \left(T^b P_i^a - T^a P_i^b\right) f, \quad (6) \end{aligned}$$

$$d_i = \left(T^b p_i^a - T^a p_i^b\right) f, \quad (7)$$

$$e_i = \left(T^b b_i^a - T^a b_i^b\right) f, \quad (8)$$

where

$$f = \frac{C^a T^b - C^b T^a}{T T^a T^b}. \quad (9)$$

For this two-reaction-channel data set, a more correct version of Eq. (3) would give the 2D background

$$B'_{ij} = \frac{1}{T^a}\left(P_i^a - P_j^a - p_i^a p_j^a\right) + \frac{1}{T^b}\left(P_i^b P_j^b - p_i^b p_j^b\right). \quad (10)$$

With some algebra (see Appendix A) we can now combine Eqs. 3, 6, 7 and 10 to get

$$B'_{ij} = B_{ij} + \frac{1}{F}\left(D_i D_j - d_i d_j\right), \quad (11)$$

where

$$F = f^2 T T^a T^b = \frac{\left(C^a T^b - C^b T^a\right)^2}{T T^a T^b}. \quad (12)$$

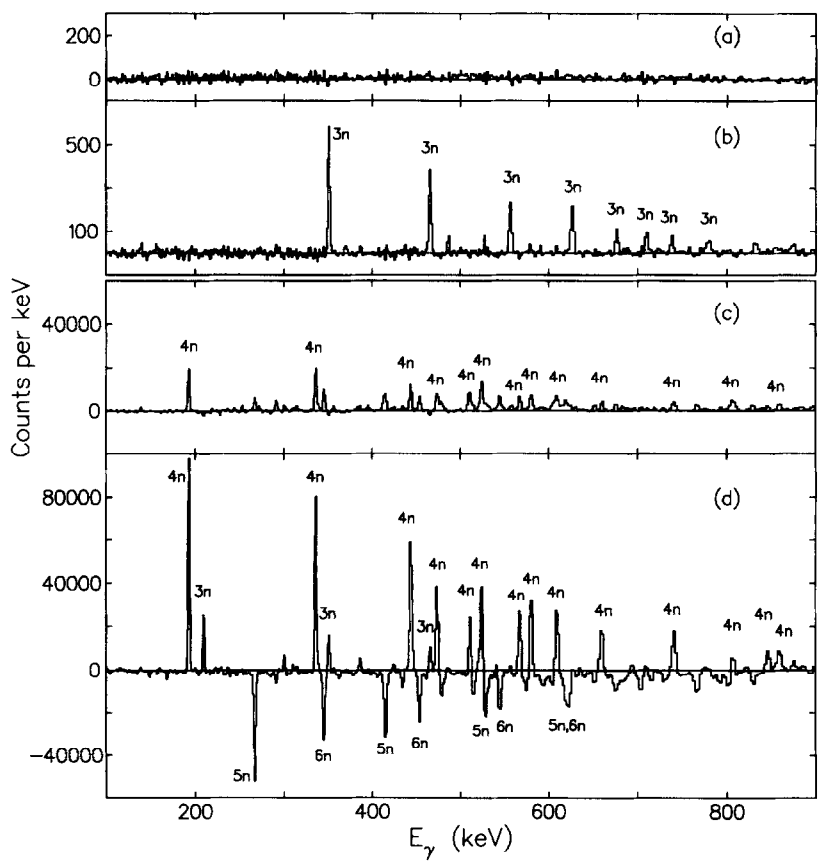

Fig. 5. (a), (b): Double-gated spectra from gates at 1340 keV and 208 keV. These transitions belong to different nuclei and are not in true coincidence. (c), (d): Spectra from a single gate set at 1340 keV. The background has been subtracted using the improved procedure of Eq. (11) ((a), (c)), or the standard procedure of Eq. (3) ((b), (d)). The data set and backgrounds are identical to those of Fig. 3 and 4. Strong peaks in the spectra are labelled by the reaction channel.

We can evaluate the constant F by taking the sum of the difference spectrum D_i over the E2-bump gate(s) E,

$$\sum_{i\in E} D_i = \sum_{i\in E} \frac{C^a T^b - C^b T^a}{T T^a T^b}\left(T^b P_i^a - T^a P_i^b\right)$$
$$= \frac{C^a T^b - C^b T^a}{T T^a T^b}\left(T^b C^a - T^a C^b\right)$$
$$= F. \qquad (13)$$

Thus we are able to eliminate the need to know the individual evaporation-residue projections in order to make use of Eq. (11).

The effect of using this improved background subtraction procedure is shown on the right-hand side of Fig. 3. The new method does not yield perfect results, especially in this case for the 6n reaction channel, presumably due to the fact that we have more than two reaction channels populated in the experiment. Nevertheless, there is a very significant improvement, especially in the region of the E2 bump.

When one sets gates on transitions in the energy range of the E2 bump, the effects of the new method are still more striking. Fig. 5 presents spectra from a single gate at 1340 keV, and from a double gate at 1340 keV and the 3n γ-ray at 208 keV, with the background subtracted using the standard procedure (Figs. 5b and 5d) or the improved procedure (Figs. 5a and 5c). The data set and backgrounds used are the same as those of Figs. 3 and 4. The 1340 keV transition belongs to the 4n reaction channel and not to the 3n channel, but it would be impossible to draw that conclusion based on Figs. 5b and 5d.

An alternative and perhaps more intuitive way of viewing this correction term is to consider the difference spectrum D_i as a gate on a matrix where the background of Eq. (3) has already been subtracted. That is,

$$D_i = \sum_{j\in E}\left(M_{ij} - B_{ij}\right)$$
$$= S_i - \frac{1}{T}\sum_{j\in E}\left(P_i P_j - p_i p_j\right)$$
$$\approx S_i - \frac{C}{T}P_i \qquad (14)$$

since the gate E is assumed to include only background channels. We then use this projection D_i and its peak and background spectra d_i, e_i in the same way as for Eq. (3), except that we also need to replace the total counts

$$T = \sum_i P_i$$

with

$$F = \sum_{i\in E} D_i.$$

This then corrects the matrix for background correlations remaining in the E2 bump after the first background subtraction. Presumably, we could repeat this procedure for a second problem area, using the matrix which has been background-subtracted with Eq. (11) and a different gate.

It should be emphasized that the problems presented by the E2-bump are not restricted to the background-subtraction method of Eq. 3. Any method that treats the background as a fraction of some spectrum (such as the total 1D projection) is prone to this problem, unless that spectrum is derived directly from background gates set close to the gate of interest. It is also worth noting that the results presented here are not very sensitive to the actual gate(s) used to generate the E2-bump projection. The main criterion is simply a sensitivity to the reaction-channel dependence of the E2 bump strength. While it is a good idea to exclude strong peaks, weak peaks such as those in Fig. 4a can be included with no observable effects.

For residual nuclei that do not exhibit strong collective rotation at the spins at which they are populated, there is no strong E2 bump. For these cases, the variation of the intensity of the E2 bump with reaction channel is not as evident, and may be absent altogether for some reactions. For example, a comparison of the gates shown in Fig. 1 with those in Fig. 3 shows that the effect is less pronounced for the noncollective nuclei ^{148,149}Gd (although a close inspection reveals that the spectrum of Fig. 1b is slightly oversubtracted in the region 1.0–1.6 MeV, and that of Fig. 1c slightly undersubtracted). In cases where no reaction-channel fractionation is observed, the use of Eq. (11) over that of Eq. (3) is not necessary, and may in fact degrade the overall quality of the background subtraction.

5. Extension to triples and higher folds

The new spectrometers such as GAMMASPHERE and EUROGAM gain increased sensitivity by making use of high-fold coincidences to increase the peak-to-background ratio for γ-ray coincidences. Since the background is reduced by more than an order of magnitude over that of double coincidences, one might conclude that background subtraction of quadruple- or quintuple-coincidence data should be less important. It must be remembered, however, that the goal of these instruments is to make use of the increased sensitivity to search for and examine transitions or cascades which are an order of magnitude weaker than those observed with earlier instruments. Thus the peak-to-background ratio at the limit of sensitivity is approximately unchanged, and the background will have to be treated properly in order to correctly extract information from the new high-fold data sets.

The procedures described here can be easily extended to triples and higher-fold coincidences. Figs. 1, 2 and 3 show results for double gates on triples data sets, obtained with the extensions to Eq. (3) and (11) that are given below. Extensions of the Palameta–Waddington technique

to triples and higher folds are derived in Ref. [7]. Crowell et al. [3] have also developed a high-fold background-subtraction algorithm which is in some respects similar to that of Eq. (15) and (16) below, except that they replace the spectrum b_i with estimates of the background levels derived directly from the high-fold data in the region of the gate. They also do not subtract the background counts in coincidence with the (n-1)-fold peak portion of the gate on n-fold data.

The extension of Eq. (3) is straightforward. We consider an n-fold cross-product of the 1D projection, keeping all terms that include at least one power of the spectrum b. For example,

$$\begin{aligned} P_iP_jP_k = {} & p_ip_jp_k \\ & + p_ip_jb_k + p_ib_jp_k + b_ip_jp_k \\ & + p_ib_jb_k + b_ip_jb_k + b_ib_jp_k \\ & + b_ib_jb_k. \end{aligned}$$

To get the three-dimensional background B_{ijk}, we drop the first term, replace the pp terms with the corresponding background-subtracted 2D projection (in order to include the proper coincidence relationships) and divide by powers of T (to get the correct dependence on the total number of events),

$$\begin{aligned} B_{ijk} = {} & \frac{1}{T}\left[\left(M_{ij}-B_{ij}\right)b_k + \left(M_{ik}-B_{ik}\right)b_j \right. \\ & \left. + \left(M_{jk}-B_{jk}\right)b_i\right] \\ & + \frac{1}{T^2}\left[p_ib_jb_k + b_ip_jb_k + b_ib_jp_k + b_ib_jb_k\right]. \end{aligned}$$

By expanding B_{ij} etc. through Eq. (3), we get

$$\begin{aligned} B_{ijk} = {} & \frac{1}{T}\left[M_{ij}b_k + M_{ik}b_j + M_{jk}b_i\right] \\ & + \frac{1}{T^2}\left[-P_ib_jb_k - b_iP_jb_k - b_ib_jP_k + b_ib_jb_k\right]. \end{aligned} \tag{15}$$

Similarly, for quadruple coincidences, we obtain

$$\begin{aligned} B_{ijkl} = {} & \frac{1}{T}\left[C_{ijk}b_l + C_{ijl}b_k + C_{ikl}b_j + C_{jlk}b_i\right] \\ & + \frac{1}{T^2}\left[-M_{ij}b_kb_l - M_{ik}b_jb_l - M_{jk}b_ib_l - M_{il}b_jb_k \right. \\ & \left. - M_{jl}b_ib_k - M_{kl}b_ib_j\right] \\ & + \frac{1}{T^3}\left[P_ib_jb_kb_l + b_iP_jb_kb_l + b_ib_jP_kb_l + b_ib_jb_kP_l \right. \\ & \left. - b_ib_jb_kb_l\right], \end{aligned} \tag{16}$$

where C_{ijk} is the three-dimensional (3D) projection of the 4-dimensional (4D) data set. For completeness, we rewrite Eq. (3) in the same form as Eq. (15) and (16),

$$B_{ij} = \frac{1}{T}\left[P_ib_j + b_iP_j - b_ib_j\right].$$

We see that in order to calculate the background, we require all of the projections of order less than the coincidence fold, in addition to the 1D background spectrum. The same is true for the extension of Eq. (11), except that in that method we also require all the E2-bump-gated projections and the corresponding 1D background spectrum.

Using the format of Eq. (15), the triples version of Eq. (11) reduces to

$$\begin{aligned} B'_{ijk} = {} & B_{ijk} + \frac{1}{F}\left[N_{ij}e_k + N_{ik}e_j + N_{jk}e_i\right] \\ & + \frac{1}{F^2}\left[-Q_ie_je_k - e_iQ_je_k - e_ie_jQ_k + \frac{U}{F}e_ie_je_k\right]. \end{aligned} \tag{17}$$

where

$$\begin{aligned} N_{ij} = {} & \sum_{k\in E}\left(C_{ijk}-B_{ijk}\right) \\ = {} & \sum_{k\in E}C_{ijk} - \frac{C}{T}M_{ij} - \frac{1}{T}\left(D_ib_j + b_iD_j\right), \end{aligned} \tag{18}$$

$$\begin{aligned} Q_i = {} & \sum_{j\in E}N_{ij} \\ = {} & \sum_{j\in E}\sum_{k\in E}C_{ijk} - \frac{1}{T}\left(CS_i + CD_i + Fb_j\right) \\ = {} & \sum_{j\in E}\sum_{k\in E}C_{ijk} - \frac{1}{T}\left(2CD_i + \frac{C^2}{T}P_i + Fb_j\right), \end{aligned} \tag{19}$$

$$\begin{aligned} U = {} & \sum_{i\in E}Q_i \\ = {} & \sum_{i\in E}\sum_{j\in E}\sum_{k\in E}C_{ijk} - \frac{1}{T}\left(3CF + \frac{C^3}{T}\right), \end{aligned} \tag{20}$$

are the E2-bump-gated projections of the background-subtracted cube. Using the arguments of the previous section and algebra similar to that of Appendix A, one can show that the correct 3D background for our data set with two reaction channels reduces to Eq. (17).

Similarly, the quadruples version of Eq. (11) is

$$\begin{aligned} B'_{ijkl} = {} & B_{ijkl} + \frac{1}{F}\left[G_{ijk}e_l + G_{ijl}e_k + G_{ikl}e_j + G_{jlk}e_i\right] \\ & + \frac{1}{F^2}\left[-O_{ij}e_ke_l - O_{ik}e_je_l - O_{jk}e_ie_l - O_{il}e_je_k \right. \\ & \left. - O_{jl}e_ie_k - O_{kl}e_ie_j\right] \\ & + \frac{1}{F^3}\left[R_ie_je_ke_l + e_iR_je_ke_l + e_ie_jR_ke_l \right. \\ & \left. + e_ie_je_kR_l - \frac{V}{F}e_ie_je_ke_l\right], \end{aligned} \tag{21}$$

where

$$G_{ijk} = \sum_{l \in E} \left(H_{ijkl} - B_{ijkl} \right),$$

$$N_{ij} = \sum_{k \in E} G_{ijk},$$

$$Q_i = \sum_{j \in E} N_{ij},$$

$$V = \sum_{i \in E} Q_i,$$

are the E2-bump-gated projections of the background-subtracted 4D data set (hypercube) H_{ijkl}.

Hackman and Waddington [7] have developed a very elegant notation of using operators to describe the process of background subtraction. In our case, the operator for the standard background subtraction is

$$\beta_i = 1 - \frac{b_i}{T} \sum_i$$

for each dimension. Thus, for example,

$$\begin{aligned} \beta_i \beta_j M_{ij} &= \left(1 - \frac{b_i}{T} \sum_i \right) \left(1 - \frac{b_j}{T} \sum_j \right) M_{ij} \\ &= M_{ij} - \frac{b_i}{T} P_j - \frac{b_j}{T} P_i + \frac{b_i}{T} \frac{b_j}{T} T \\ &= M_{ij} - B_{ij}. \end{aligned}$$

Similarly,

$$\beta_i \beta_j \beta_k C_{ijk} = C_{ijk} - B_{ijk}$$

etc. The operator to apply the additional E2-bump correction is

$$\epsilon_i = 1 - \frac{e_i}{F} \sum_i$$

for each dimension, so that

$$\epsilon_i \epsilon_j \beta_i \beta_j M_{ij} = M_{ij} - B'_{ij},$$

$$\epsilon_i \epsilon_j \epsilon_k \beta_i \beta_j \beta_k C_{ijk} = C_{ijk} - B'_{ijk},$$

etc.

One final remark should be made about background subtraction for triples and higher-fold data. We have assumed throughout the discussion here that the quasicontinuum part of the background is uncorrelated, that is, that the 2D background–background coincidences are well-described by the tensor cross-product of the 1D background spectrum b_i (with the exception of the E2 bump). While this turns out to be a reasonable approximation, it has long been known (e.g. Ref. [6]) that there is often a valley along the diagonals of the data; events where $E_{\gamma 1} \approx E_{\gamma 2}$ are slightly less likely than expected from uncorrelated backgrounds. For 2D data, this problem can be alleviated to some extent by using local backgrounds.

This valley is even deeper along the major diagonal ($E_{\gamma 1} \approx E_{\gamma 2} \approx E_{\gamma 3}$) in triples data, so at first it might be expected that the 3D background from the prescriptions described in this paper would be poorer in this respect than that for 2D data. This, however, turns out not to be the case. Referring to Eq. (15), one sees that the 2D correlations for $i \approx j$, $i \approx k$ and $j \approx k$ are included in the terms $M_{ij} b_k$, $M_{ik} b_j$ and $M_{jk} b_i$, respectively. Experience indicates that these terms tend to cancel the background correlations in the γ–γ–γ cube.

6. Conclusion

Background-subtraction algorithms for in-beam HPGe coincidence data have been presented. The backgrounds are parameterized as the cross-products of lower-dimensional projections of the data and a one-dimensional background spectrum. A novel method of correcting for a mixture of different reaction channels in the complete data set is described. This method makes use of one or more gates on background channels in the energy region of the "E2 bump", and provides a significantly better description of the background for nuclei exhibiting strong collective rotation at high spins.

The prescriptions for background subtraction described here are simple, fast and reliable. The results seem to be reasonably insensitive to the particulars of the chosen background spectra and to the gate used to generate the E2-bump correction terms.

Acknowledgements

I thank John Simpson, Mark Riley and co-workers for the use of the EUROGAM 1 data set from the reaction of ^{114}Cd with 210 MeV ^{48}Ca, and G. Hackman and J.C. Waddington for very helpful discussions.

Appendix A. Algebra for the E2-bump correction in two dimensions

We have (from Eq. (10))

$$\begin{aligned} B'_{ij} &= \frac{1}{T^{\mathrm{a}}} \left(P_i^{\mathrm{a}} P_j^{\mathrm{a}} - p_i^{\mathrm{a}} p_j^{\mathrm{a}} \right) + \frac{1}{T_{\mathrm{b}}} \left(P_i^{\mathrm{b}} P_j^{\mathrm{b}} - p_i^{\mathrm{b}} p_j^{\mathrm{b}} \right) \\ &= B_{ij} + \frac{1}{T_{\mathrm{a}}} P_i^{\mathrm{a}} P_j^{\mathrm{a}} + \frac{1}{T^{\mathrm{b}}} P_i^{\mathrm{b}} P_j^{\mathrm{b}} - \frac{1}{T} P_i P_j - \frac{1}{T^{\mathrm{a}}} p_i^{\mathrm{a}} p_j^{\mathrm{a}} \\ &\quad - \frac{1}{T^{\mathrm{b}}} p_i^{\mathrm{b}} p_j^{\mathrm{b}} + \frac{1}{T} p_i p_j. \end{aligned}$$

Collecting the terms of type PP together and making use of Eqs. (6), (9) and (12), we get

$$\begin{aligned}
&\frac{1}{T^{\mathrm{a}}}P_i^{\mathrm{a}}P_j^{\mathrm{a}} + \frac{1}{T^{\mathrm{b}}}P_i^{\mathrm{b}}P_j^{\mathrm{b}} - \frac{1}{T}P_iP_j \\
&= \frac{1}{T^{\mathrm{a}}}P_i^{\mathrm{a}}P_j^{\mathrm{a}} + \frac{1}{T^{\mathrm{b}}}P_i^{\mathrm{b}}P_j^{\mathrm{b}} - \frac{1}{T}P_i^{\mathrm{a}}P_j - \frac{1}{T}P_i^{\mathrm{b}}P_j \\
&= \frac{1}{TT^{\mathrm{a}}}P_i^{\mathrm{a}}\left(TP_j^{\mathrm{a}} - T^{\mathrm{a}}P_j\right) + \frac{1}{TT^{\mathrm{b}}}P_i^{\mathrm{b}}\left(TP_j^{\mathrm{b}} - T^{\mathrm{b}}P_j\right) \\
&= \frac{1}{TT^{\mathrm{a}}}P_i^{\mathrm{a}}\left(T^{\mathrm{b}}P_j^{\mathrm{a}} - T^{\mathrm{a}}P_j^{\mathrm{b}}\right) + \frac{1}{TT^{\mathrm{b}}}P_i^{\mathrm{b}}\left(T^{\mathrm{a}}P_j^{\mathrm{b}} - T^{\mathrm{b}}P_j^{\mathrm{a}}\right) \\
&= \frac{1}{fTT^{\mathrm{a}}}P_i^{\mathrm{a}}D_j - \frac{1}{fTT^{\mathrm{b}}}P_i^{\mathrm{b}}D_j \\
&= \frac{1}{fTT^{\mathrm{a}}T^{\mathrm{b}}}\left(T^{\mathrm{b}}P_i^{\mathrm{a}} - T^{\mathrm{a}}P_i^{\mathrm{b}}\right)D_j \\
&= \frac{1}{f^2TT^{\mathrm{a}}T^{\mathrm{b}}}D_iD_j \\
&= \frac{1}{F}D_iD_j.
\end{aligned}$$

Similarly, collecting the terms of type pp together, we have

$$\frac{1}{T^{\mathrm{a}}}p_i^{\mathrm{a}}p_j^{\mathrm{a}} + \frac{1}{T^{\mathrm{b}}}p_i^{\mathrm{b}}p_j^{\mathrm{b}} - \frac{1}{T}p_ip_j = \frac{1}{F}d_id_j$$

and thus

$$B'_{ij} = B_{ij} + \frac{1}{F}\left(D_iD_j - d_id_j\right).$$

References

[1] M. Bergström and P. Ekström, Nucl. Instr. and Meth. A 301 (1991) 132.

[2] D.C. Radford, Nucl. Instr. and Meth. A, accompanying paper.

[3] B. Crowell, M.P. Carpenter, R.G. Henry, R.V.F. Janssens, T.L. Khoo, T. Lauritsen and D. Nisius, to be published in Nucl. Instr. and Meth. A.

[4] G. Palameta and J.C. Waddington, Nucl. Instr. and Meth. A 234 (1985) 476.

[5] S. Flibotte et al., Phys. Rev. Lett 71 (1993) 688.

[6] O. Andersen, J.D. Garrett, G.B. Hagemann, B. Herskind, D.L. Hillis and L.L. Riedinger, Phys. Rev. Lett. 43 (1979) 687; B. Herskind, J. Phys. (Paris) 41 (1980) C10-106.

[7] G. Hackman and J.C. Waddington, to be published in Nucl. Instr. and Meth. A.